Research Article | Vol. 25, No. 10 | 15 May 2017 | OPTICS EXPRESS 10925

Optics EXPRESS

# Interferometric space-mode multiplexing based on binary phase plates and refractive phase shifters

JESÚS LIÑARES, XESÚS PRIETO-BLANCO,* VICENTE MORENO, CARLOS MONTERO-ORILLE, DOLORES MOURIZ, MARÍA C. NISTAL AND DAVID BARRAL

*Optics area, Department of Applied Physics, Faculty of Physics / Faculty of Optics and Optometry, Universidade de Santiago de Compostela, Campus Vida s/n, E-15782 Santiago de Compostela, Galicia, Spain*

*xesus.prieto.blanco@usc.es

**Abstract:** A Mach-Zehnder interferometer (MZI) that includes in an arm either a reflective image inverter or a Gouy phase shifter (RGPS) can (de)multiplex many types of modes of a few mode fiber without fundamental loss. The use of RGPSs in combination with binary phase plates for multiplexing purposes is studied for the first time, showing that the particular RGPS that shifts $\pi$ the odd modes only multiplexes accurately low order modes. To overcome such a restriction, we present a new exact refractive image inverter, more compact and flexible than its reflective counterpart. Moreover, we show that these interferometers remove or reduce the crosstalk that the binary phase plates could introduce between the multiplexed modes. Finally, an experimental analysis of a MZI with both an approximated and an exact refractive image inverter is presented for the case of a bimodal multiplexing. Likewise, it is proven experimentally that a RGPS that shifts $\pi/2$ demultiplexes two odd modes which can not be achieved by any image inverter.



**OCIS codes:** (060.0060) Fiber optics and optical communications, (060.2340) Fiber optics components, (060.4230) Multiplexing, (050.5080) Phase shift, (110.2760) Gradient-index lenses.

## References and links

1. G. Li, N. Bai, N. Zhao, and C. Xia, "Space-division multiplexing: the next frontier in optical communication," Adv. Opt. Photon. **6**, 413–487 (2014).
2. N. Bai, E. Ip, Y.-K. Huang, E. Mateo, F. Yaman, M.-J. Li, S. Bickham, S. Ten, J. Liñares, C. Montero, V. Moreno, X. Prieto, V. Tse, K. M. Chung, A. P. T. Lau, H.-Y. Tam, C. Lu, Y. Luo, G.-D. Peng, G. Li, and T. Wang, "Mode-division multiplexed transmission with inline few-mode fiber amplifier," Opt. Express **20**, 2668–2680 (2012).
3. D. Soma, K. Igarashi, Y. Wakayama, K. Takeshima, Y. Kawaguchi, N. Yoshikane, T. Tsuritani, I. Morita, and M. Suzuki, "2.05 Peta-bit/s super-nyquist-WDM SDM transmission using 9.8-km 6-mode 19-core fiber in full C band," in "2015 European Conference on Optical Communication (ECOC)," (2015), pp. 1–3.
4. Y. Weng, E. Ip, Z. Pan, and T. Wang, "Advanced spatial-division multiplexed measurement systems propositions—from telecommunication to sensing applications: A review," Sensors **16**, 1387 (2016).
5. C. Montero-Orille, V. Moreno, X. Prieto-Blanco, E. F. Mateo, E. Ip, J. Crespo, and J. Liñares, "Ion-exchanged glass binary phase plates for mode-division multiplexing," Appl. Opt. **52**, 2332–2339 (2013).
6. H. Wei, X. Xue, J. Leach, M. J. Padgett, S. M. Barnett, S. Franke-Arnold, E. Yao, and J. Courtial, "Simplified measurement of the orbital angular momentum of single photons," Opt. Commun. **223**, 117 – 122 (2003).
7. P. Boffi, P. Martelli, A. Gatto, and M. Martinelli, "Mode-division multiplexing in fibre-optic communications based on orbital angular momentum," Journal of Optics **15**, 075403 (2013).
8. H. Huang, G. Milione, M. P. J. Lavery, G. Xie, Y. Ren, Y. Cao, N. Ahmed, T. An Nguyen, D. A. Nolan, M.-J. Li, M. Tur, R. R. Alfano, and A. E. Willner, "Mode division multiplexing using an orbital angular momentum mode sorter and MIMO-DSP over a graded-index few-mode optical fibre," Sci. Rep. **5**, 14931 (2015).
9. K. Igarashi, D. Souma, K. Takeshima, and T. Tsuritani, "Selective mode multiplexer based on phase plates and Mach-Zehnder interferometer with image inversion function," Opt. Express **23**, 183–194 (2015).
10. J. Liñares, X. Prieto-Blanco, C. Montero-Orille, and V. Moreno, "Spatial mode multiplexing/demultiplexing by Gouy phase interferometry," Opt. Lett. **42**, 93–96 (2017).
11. J. Liñares and C. Gómez-Reino, "Diffraction-limited coupling efficiency between SMF connected by GRIN fibre lens," J. Mod. Opt **38**, 597–604 (1991).

#286779 https://doi.org/10.1364/OE.25.010925
Journal © 2017 Received 16 Feb 2017; revised 20 Apr 2017; accepted 23 Apr 2017; published 3 May 2017

Optics EXPRESS

12. J. Liñares, X. Prieto-Blanco, C. Montero, V. Moreno, E. F. Mateo, M. D. Mouriz, and M. C. Nistal, "Mode-division multiplexing by Mach-Zehnder interferometers with graded-index elements," in "Proceedings of IX Optoelectronics Spanish Meeting," (Salamanca, 2015), pp. PO–SII–07.
13. J. von Hoyningen-Huene, R. Ryf, and P. Winzer, "LCoS-based mode shaper for few-mode fiber," Opt. Express **21**, 18097–18110 (2013).
14. A. Belafhal and L. Dalil-Essakali, "Collins formula and propagation of Bessel-modulated Gaussian light beams through an ABCD optical system," Opt. Commun. **177**, 181 – 188 (2000).
15. I. Kimel and L. R. Elias, "Relations between Hermite and Laguerre Gaussian modes," IEEE J. Quantum Electron. **29**, 2562–2567 (1993).
16. M. Beijersbergen, L. Allen, H. van der Veen, and J. Woerdman, "Astigmatic laser mode converters and transfer of orbital angular momentum," Opt. Commun. **96**, 123 – 132 (1993).
17. R. Brüning, Y. Zhang, M. McLaren, M. Duparré, and A. Forbes, "Overlap relation between free-space Laguerre Gaussian modes and step-index fiber modes," J. Opt. Soc. Am. A **32**, 1678–1682 (2015).
18. A. A. Tovar and L. W. Casperson, "Generalized reverse theorems for multipass applications in matrix optics," J. Opt. Soc. Am. A **11**, 2633–2642 (1994).
19. J. W. Goodman, *Introduction to Fourier Optics* (Roberts and Company Publishers, 2005), 3rd ed.

## 1. Introduction

The multiplexing/demultiplexing of spatial modes in few mode optical fibers (FMF) and multicore optical fibers (MCF) is an emerging operation in optical communications, optical sensors, optical information processing and so on. In optical fiber communications, it is considered as an efficient strategy to increase the network capacity [1]; in fact, several Pbit/s transmission rate can be achieved [2, 3]. Moreover space mode multiplexing is also an emerging area in the fields of optical sensors, image processing and so on [4]. Devices that implement such a strategy are spatial multiplexers, which in a first stage perform conversion to LP modes, and in a second stage combine and couple them to FMFs. Importantly, mode multiplexing is compatible with MCFs, because each core can support several modes like a FMF does. Binary phase plates (BP) which introduce a $\pi$ phase shift in selected zones of the wavefront are often used as converters. In particular $\mathrm{BP}_{lp}$ are designed to generate the phase of $\mathrm{LP}_{lp}$ modes, but not their amplitude. Therefore unwanted optical modes also emerge from the plates, which can lead to crosstalk. We consider monolithic BPs made by selective ion exchange in glass [5] because of the excellent uniformity and accuracy of their phase shift. In fact they have been used both to multiplex several signals in a FMF and to amplify them in a equalized way by coupling the pump in a particular mode of a doped FMF [2]. The second stage of the multiplexing process can be performed with beam splitters, but this produces a 3dB loss to multiplex two modes and again 3db for demultiplex them. In general, the recovered power in a $N$ mode multiplexing is, at most, $1/N^2$ times the input power. As such reduction of the signal-to-noise ratio degrades the bit error rate, several solutions have been proposed. For example, it is possible to multiplex modes with different values of the orbital angular momentum (OAM) by using cascaded mode sorters. Each sorter is a lossless Mach-Zehnder interferometer (MZI) having two Dove prisms [6, 7]. Similarly, Huang *et al.* [8] demonstrated a non interferometric OAM mode sorter based on two custom refractive optical elements that geometrically transform log-polar coordinates to Cartesian coordinates. However all these OAM multiplexers waste radial modes, so the core size quickly increases with $N$. On the other hand, Igarashi *et al.* [9] have recently proposed to multiplex the first five spatial modes without fundamental loss. They also use cascaded MZI, but in this case each of them comprises a reflective image inverter in one arm to combine an odd mode with an even one. Likewise, refractive Gouy phase shifters (RGPS) can be used instead of the reflective inverter to also multiplex modes two odd modes or two even modes [10]. However phase plates can introduce relevant crosstalk between modes with same parity. The effect of these unwanted modes in RGPSs has not yet been studied.

We propose to use selective phase shifters based on either RGPS or refractive image inversion shifters (RIIS) according to the kind of modes to be multiplexed, taking into account the undesired

Optics EXPRESS

modes generated by the phase plates. All of these phase shifters consist of refractive elements appropriately arranged, such as conventional lenses and/or micro-optic elements as graded-index lenses or fiber lenses [11]. As to practical advantages of refractive phase shifters, we underline their simpler alignment, polarization insensitivity, a selective action in both directions of the space by using cylindrical lenses and even a higher compatibility with optical fibers by using micro-optic elements, as recently shown [10, 12]. Note that a reflective inverter increases notably the optical path of one arm which must be compensated with a detour in the other arm including two extra mirrors. Accordingly, more compact and smaller refractive interferometric multiplexers can be implemented. As to conceptual advantages, we stress that RGPSs allow for multiplexing optical modes regardless parity or separability of the functions representing the modal amplitude; particularly, two even (or two odd) LP modes can only be multiplexed by RGPSs. However, RGPSs will present difficulties for multiplexing any even mode with some odd mode. On the contrary, RIISs does not have such problems and they do not impose any constraint to the curvature wavefront or waist size, unlike RGPSs. Nevertheless, image inverters can only multiplex modes with different parity (in one or two directions). Therefore, the combination of both kind of phase shifters allows for the multiplexing of a large number of optical modes.

The structure of the paper is as follows. In section 2 we present the theory and design of interferometric multiplexers based on RGPSs and describe their advantages for multiplexing modes produced by $BP_{0p}$ plates. We also explain their limitations when they are used for multiplexing modes with opposed parity. In section 3 we describe interferometric multiplexers based on both RIISs and $BP_{l1}$ generating optical fields close to $LP_{l1}$ modes. In section 4 we present and analyze the experimental results obtained for the case of a MZI with a RIIS. In section 5 conclusions are presented.

## 2. Refractive Gouy phase shifters

In this section we present, by one hand, the spatial propagation of optical modes to be multiplexed. Although there are several kind of optical modes we restrict our attention to Hermite-Gaussian (HG) modes. These modes form a complete set of functions and are especially suitable to study cylindrical systems because of its separability. On the other hand, we describe how a RGPS works within a MZI. Finally, we present the multiplexing of $LP_{0p}$ modes, that is, modes with rotational symmetry whose generation with BPs is particularly efficient [13].

### 2.1. Optical beam propagation

The method proposed in this section can be applied to different kind of $F$-Gaussian optical beams, such as Laguerre-Gaussian (LG), Ince-Gaussian, Bessel-Gaussian, and so on. These optical beams can come from the LP modes of a FMF, that is, $\xi_{lp(c,s)}(r,\varphi) = F_{lp}(r)\exp\{-r^2/w_0^2\}(\cos l\varphi, \sin l\varphi)$. However, for the reasons stated above and without loss of generality, we will consider the important set of Hermite-Gaussian optical modes. First, let us consider briefly the propagation of HG optical modes of order $m, n = 0, 1, 2, \ldots$, through an optical system $A_iB_iC_iD_i$, where subindex $i$ stands for the arm of the interferometer followed by the beam. Let us also consider HG optical modes $\Upsilon_{mn}(\boldsymbol{\rho}_0)$, with $\boldsymbol{\rho}_0 = (x_0, y_0)$, at the plane of a waist, then the optical beam, after propagation through the path $i$, at the exit of the optical system is given by the expression

$$\Upsilon_{mni}(\boldsymbol{\rho}) = \int\int K_i(\boldsymbol{\rho}, \boldsymbol{\rho}_0)\Upsilon_{mn}(\boldsymbol{\rho}_0)d\boldsymbol{\rho}_0, \tag{1}$$

with $\boldsymbol{\rho} = (x, y)$ and $K_i(\boldsymbol{\rho}, \boldsymbol{\rho}_0)$ the optical propagator given by

$$K_i(\boldsymbol{\rho}, \boldsymbol{\rho}_0) = \frac{ik_0}{2\pi B_i}\exp\left\{\frac{ik_0}{2B_i}\left[D_i(x^2+y^2) + A_i(x_0^2+y_0^2) - 2xx_0 - 2yy_0\right]\right\}, \tag{2}$$

Optics EXPRESS

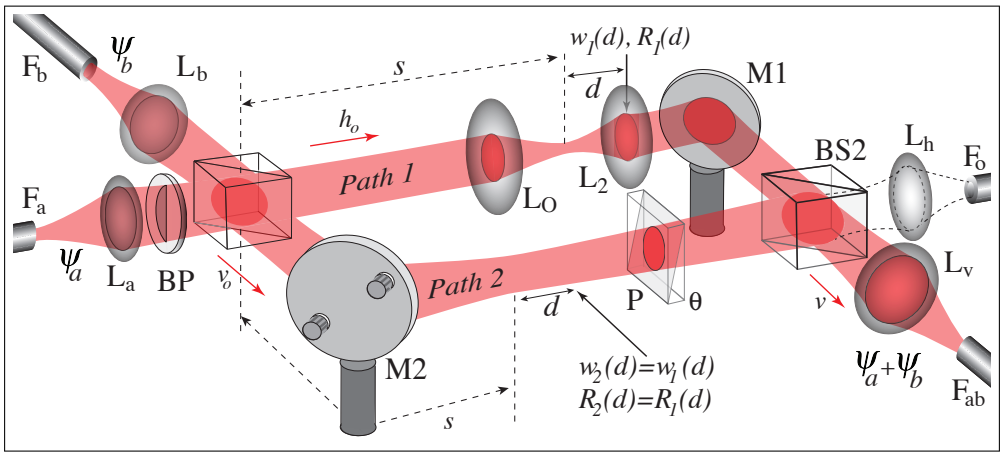


Fig. 1. MZI for implementing relative Gouy phases and multiplexing.

therefore, by performing the above integral we obtain the HG optical beam

$$\Upsilon_{mni}(x,y) = \frac{C_{mni}}{w_i} H_m\left(\frac{x}{\sqrt{2}w_i}\right) H_n\left(\frac{y}{\sqrt{2}w_i}\right) \exp\left(-\frac{x^2+y^2}{w_i^2}\right) \exp\left(\mathrm{i}k_0 \frac{x^2+y^2}{2R_i}\right) \exp(-\mathrm{i}\phi_{mni}), \tag{3}$$

with $C_{mni}$ a complex constant (not relevant in our analysis) and $k_0$ the wavenumber in vacuum. Moreover, $w_i$, the half-width of the Gaussian function, $R_i$, the curvature radius of the wavefronts, and $\phi_{mni}$, the Gouy phase, are giving by the following expressions [11, 14]:

$$w_i^2 = \frac{w_{oi}^2}{z_{Ri}^2}\left(z_{Ri}^2 A_i^2 + B_i^2\right), \qquad \frac{1}{R_i} = \frac{w_{oi}^2}{w_i^2}\left[A_i C_i + \frac{B_i D_i}{z_{Ri}^2}\right], \tag{4}$$

$$\phi_{mni} = (m+n+1)\arctan\left(\frac{B_i}{z_{Ri}A_i}\right), \tag{5}$$

with $z_{Ri} = \pi w_{oi}^2/\lambda_0$ the Rayleigh length and $w_{oi}$ the half-width at the input of the system. Note that at the input plane, the ABCD matrix is the identity and the curvature $1/R_i$ cancels. We stress that the above expressions for $w_i$ and $R_i$ are identical for many optical beams such as Laguerre-Gaussian (LG) beams. Moreover, it is important to underline that LG beams can be expressed in turn as a linear combination of HG optical beams of the same order. Indeed, by denoting the LG modes as $\Psi_{\nu\mu}$, with $l = |\nu - \mu|$, $p = \min\{\nu, \mu\}$, we can write [15]

$$\Psi_{\nu\mu(c,s)}(x,y) = \sum_{(j\ \text{even},\ j\ \text{odd})}^{\nu+\mu} \frac{\mathrm{i}^{(j,j-1)}}{2} C_{\nu\mu,j}\Upsilon_{\mu+\nu-j,j}(x,y), \tag{6}$$

with $C_{\nu\mu,j}$ real coefficients [16], $\nu \geq \mu$ and where the subindex $i$ has been removed for clarity's sake. The subindices $(c,s)$ correspond to $j$ even and $j$ odd, respectivley, and indicate that LG modes have azimuthal dependence $\cos l\varphi$ and $\sin l\varphi$. Thus, given a LG mode we can calculate and analyze, for example, its Gouy phase since it can be expressed as a linear combination of HG modes of the same order.

### 2.2. MZI multiplexer with RGPSs and their limits

We start by considering a MZI as shown in Fig. 1. A phase plate BP, lenses $L_a$, $L_b$ and optical fibers $F_a$ and $F_b$ are placed at the MZI inputs; similarly, lenses $L_h$, $L_v$ and optical fibers $F_o$ and

Optics EXPRESS

$F_{ab}$ are located at the outputs. In one of the paths (path 1) we have a symmetric optical system to implement a RGPS, as for example, two spherical lenses $L_0$ and $L_2$m where the subindexes will be evident later. Both of them have a focal length $f$ and they are separated by a distance $2d$. In the other path (path 2) there is a second optical system as, for example, a $2d$ long free space. We assume that each optical system has its center at a distance $s$ from the first Beam-Splitter (BS1) measured along the optical axis of the respective beam. Likewise, a prism introducing a phase $\theta$ is inserted in path 2 to balance properly the MZI outputs. We are interested in a maximum constructive interference at one of the outputs and no light at the other. To that end, half-width and curvature of both beams have to match each other at BS2, or equivalently, at the exit of the optical systems. These conditions determinate the half-width and convergence of the beam at BS1 in such a way that the waists are located at the center of their respective systems, that is, at a distance $s$ from BS1 [10]. In other words, both optical systems and their beams are symmetrical. The appropriate convergence of the beams coming from the optical fibers is provided by the lenses at the inputs of the MZI. In a graphical way the following condition es fulfilled (see Fig. 1) $w_1(d) = w_2(d)$ and $R_1(d) = R_2(d)$ being $w_1(d)$ and $R_1(d)$ measured just after the lens $L_2$. Let us consider that two incoherent optical beams $\Psi_a$ and $\Psi_b$, of the same frequency, enter the interferometer along horizontal ($h_0$) and vertical ($v_0$) inputs, respectively. The interference at the MZI outputs depends on the Gouy phase at each arm, which in turn depends on the mode order. According to Eq. (5) the interferometric Gouy phase is: $\Phi_{mn} = 2(\phi_{mn1} - \phi_{nm2})$, where the factor 2 takes into account the symmetry of the optical systems. As we want $\Psi_b$ to exit totally by the $v$ port, we must adjust properly the mode-insensitive phase shifter $\theta$, implemented by a thin element such as a single or double prism. Now, if the mode $\Psi_a$ is the same as $\Psi_b$ (for example, in absence of BP), thermodynamics states that $\Psi_a$ will necessarily emerge from the opposite exit that $\Psi_b$. However, if the order $m_a + n_a$ of $\Psi_a$ is different from that of $\Psi_b$, then we can arrange the optical systems in order to make the difference between interferometric Gouy phases of each beam ($\Phi_{m_a n_a} - \Phi_{m_b n_b}$) equal to $\pi$. Consequently, both modes will emerge from the same exit, performing the multiplexing operation.

As the BP is in a region where the beam convergence is low, its position along the beam is almost irrelevant. However the BP also can be placed between the fiber and the lens, where the beam width changes with propagation. Thus its position along propagation axis can be used to optimize the coupling to the desired mode by fine tuning the ratio between the beam width and the BP size. Note that if the BP couples a part of the beam $\Psi_a$ to the same HG mode as $\Psi_b$ (that is, crosstalk occurs), then that part will interfere destructively at the $v$ port: the interferometer removes the crosstalk that the plate can generate between the input HG modes. The same thing happens to LG modes, as we will show in an example. If the exit fiber is of step-index type, there will be a coupling between LG and LP modes which will introduce a slight crosstalk between some LP modes. However this will be much lower than the plate crosstalk [17]. Even better, if we use a proper gradient-index output fiber, the LG propagation modes can be directly coupled to the fiber modes and the crosstalk from the plate is removed by the MZI. It seems that authors of previous works have not noticed this useful behavior.

Next, we present two particular implementations of RGPS by using conventional lenses and graded-index lenses.

#### 2.2.1. RGPS with conventional lenses

We start by applying the Eq. (5) for the second half of the optical systems, that is, a $d$ long free space and a lens of focal $f$ in the first arm ($A_1 = 1$, $B_1 = d$, $C_1 = -1/f$ and $D_1 = 1 - d/f$) and just a $d$ long free space in the second arm ($A_2 = 1$, $B_2 = d$, $C_2 = 0$ and $D_2 = 1$). The Gouy phase for the whole interferometer is then given by

$$\Phi_{mn} = (m + n + 1)\, 2 \arctan\left[\frac{(z_{R2} - z_{R1})d}{z_{R2} z_{R1} + d^2}\right]. \tag{7}$$

Optics EXPRESS

where $z_{Ri}$ must fulfill $z_{R1} = \kappa d$ and $z_{R2} = d/\kappa$, with $\kappa = [(f-d)/(f+d)]^{1/2}$, in order for the half-widths and curvatures of both beams to match at BS2, that is, $w_1(d) = w_2(d)$ and $R_1(d) = R_2(d)$. This simplifies the Eq. (7) to [10]:

$$\Phi_{mn} = (m+n+1)\,\Delta\phi \quad \text{with} \quad \Delta\phi = 2\arcsin(d/f). \tag{8}$$

The corresponding RGPS is denoted as $G(\Delta\phi)$, but we are only interested in those that fulfill $\Delta\phi = \pi/\sigma$, with $\sigma = 1, 2, 3\ldots$ since they allow for multiplexing. Thus $G(\pi)$, $G(\pi/2)$, $G(\pi/3)$, $G(\pi/4)\ldots$ are implemented if $d/f = 1$, $\sin(\pi/4)$, $\sin(\pi/6)$, $\sin(\pi/8)\ldots$ The first case, $d = f$, presents a serious limitation. It defines a confocal device with $z_{R1} = 0$ and $z_{R2} = \infty$; but these conditions, as well as $\Delta\phi = \pi$, are only obtained for an infinite entrance beam diameter [16]. For a finite beam, by taking into account Eq. (7) and after a certain calculation, the Gouy phase can be written as

$$\Phi_{mn} \approx (m+n+1)\,(\pi - \epsilon) \quad \text{with} \quad \epsilon = 4z_{R1}/d\,. \tag{9}$$

Note that the deviation of the phase from the value $\pi$ increases with the mode order. Thus, when many HG modes are needed to represent an optical beam then the $G(\pi)$ shifter can give rise to important deviations from the exact behavior. For example, if this shifter is used for multiplexing by BPs, the diffracted field generated by the plate can be complex enough to need a high number of HG modes to be represented properly. In this case, an alternative multiplexing system should be used. The goal would be to produce a relative phase exactly equal to $\pi$, that is, an inversion of odd functions. Therefore, a refractive image inverter can be used. We leave its detailed study for the next section.

Finally, we can also consider one-dimensional optical systems in one arm of the MZI, that is, optical systems such as cylindrical lenses acting only on one direction $\eta = x$ or $y$ (active direction). In this case the interferometric Gouy phase of unidimensional HG modes is given, by taking into account Eq. (7), by the expression

$$\Phi_q = \left(q + \frac{1}{2}\right)\Delta\phi\,, \tag{10}$$

with $q \equiv m, n$, for the $x$ and $y$ active directions of the optical system. The corresponding Gouy phase shifters are denoted as $G_\eta(\Delta\phi)$. Once more, these shifters present the same drawbacks above commented when BPs are used.

#### 2.2.2. RGPS with graded-index lenses

As also commented, graded-index lenses and optical fibers present a high compatibility. This allows the manufacture of compact systems and therefore justifies their study for implementing RGPSs. It is worthwhile to show how we can use the above results to design other RGPSs also based on symmetric optical systems. The ABCD matrix of such symmetric optical systems can formally be written as follows [18]

$$M = \begin{pmatrix} \cos\alpha & \frac{1}{a}\sin\alpha \\ -a\sin\alpha & \cos\alpha \end{pmatrix}, \tag{11}$$

that is, they are characterized by two independent parameters. On the other hand, an optical system formed by two spherical lenses with focal $f$ and separated a distance $2d$ has the matrix

$$M = \begin{pmatrix} 1-2d/f & 2d \\ -(2/f)(1-d/f) & 1-2d/f \end{pmatrix}. \tag{12}$$

By comparing the elements of the above matrices we obtain the following optical parameters

$$a = 2(f/d-1)^{1/2}/f, \qquad \cos\alpha = 1 - 2d/f. \tag{13}$$

Optics EXPRESS

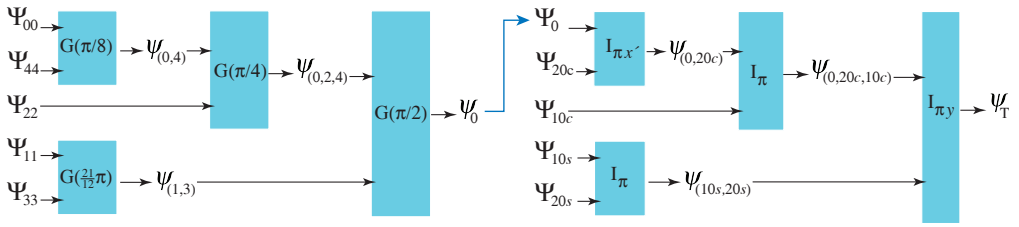


Fig. 2. Protocol of nine space mode multiplexing.

A graded-index lens (or fiber lens) [11] with length $l$, gradient parameter $g_0$ and base index $n_0$ also presents a mirror symmetry at $z = l/2$, thus its optical matrix can take the form of Eq. (11). Indeed, we simply have to take $\alpha = g_0 l$ and $a = n_0 g_0$. Therefore, from Eq. (13) we obtain a graded-index lens equivalent to a given RPGS with conventional lenses. Even more, by using the Eq. (8), the ratio $d/f$ can be replaced with a function of $\Delta\phi$ to obtain the $g_0 l$ value that we need for a given interferometric Gouy phase:

$$\sin^2(g_0 l/2) = \sin(\Delta\phi/2)\,. \tag{14}$$

The parameter $n_0 g_0$ is free because it also depends on $f$. The case $\Delta\phi = \pi$ corresponds to a graded index lens of half pitch length ($g_0 l = \pi$) which presents similar problems to its equivalent with conventional lenses. If we use this lens with a finite width beam, it produces a phase $\pi$ in path 1, but the emerging beam does not match the other beam which, in addition, has a non-zero phase. It suggests that additional elements would be required as shown in next section.

### 2.3. *Multiplexing of rotational symmetry LG modes*

In order to make clear the above results, let us consider the case of Laguerre-Gaussian modes of order $0p$, with $p = 0, 1, 2, 3, 4$, that is, $\nu\mu = 00,\ 11,\ 22,\ 33,\ 44$. Note that rotational symmetry BPs produce better coupling efficiency than plates with angular phase steps. We present the main steps for multiplexing all these modes (see left side of Fig. 2). The first mode is $\Psi_{00} \propto \Upsilon_{00}$, and the others can be expressed as a linear combination of HG modes, that is,

$$\Psi_{11} \propto \Upsilon_{20} + \Upsilon_{02}; \qquad \Psi_{22} \propto \Upsilon_{40} + 2\Upsilon_{22} + \Upsilon_{04}, \tag{15}$$

and similar expressions can be found for the modes $\Psi_{33}$ and $\Psi_{44}$, that is, according to Eq. (6) these modes can be written as linear combinations of even HG modes of order 6 and 8, respectively. We observe that there are two kind of modes: modes with even orders (00, 22, 44) and modes with odd orders (11, 33). First of all, we multiplex the modes of each kind and next multiplex all of them. By taking into account Eq. (8), and by a simple inspection, we can check that $G(\pi/8)$ allow us to multiplex the modes $\Psi_{00}$ and $\Psi_{44}$, that is, $\Phi_{00} = \pi/8$ and $\Phi_{44} = \pi + \pi/8$, therefore a compensating phase $\theta = -\pi/8$ is required and the optical field $\psi_{(0,4)} = \Psi_{00} + \Psi_{44}$ is obtained. Next we use a $G(\pi/4)$ and the above optical field acquires a phase $\pi/4 \pmod{2\pi}$, whereas the mode $\Psi_{22}$ accumulates a phase $\Phi_{22} = \pi + \pi/4$; so $\theta = -\pi/4$ and therefore we obtain $\psi_{(0,2,4)} = \Psi_{00} + \Psi_{22} + \Psi_{44}$. On the other hand, we have to multiplex modes 11 and 33. In this case a simple inspection is not enough and a more formal derivation is needed. Again, by taking into account Eq. (8) we can impose the following obvious conditions on the Gouy phases of these modes,

$$3\Delta\phi - \theta = (2s_1 + 1)\pi; \quad 7\Delta\phi - \theta = 2s_2\pi, \tag{16}$$

where $s_1$ and $s_2$ are integers. By choosing $s_1 = s_2 = 1$ we obtain the following values, $\theta = -15\pi/4$ and $\Delta\phi = \pi - 15\pi/12$. Therefore, we need a shifter $G(21\pi/12)$, so that $\Phi_{11} = 3\pi$ and

Optics EXPRESS

$\Phi_{33} = 2\pi$, and accordingly we obtain $\psi_{(1,3)} = \Psi_{11} + \Psi_{33}$. Finally, we have to multiplex the optical fields $\psi_{(1,3)}$ and $\psi_{(0,2,4)}$. It is important to indicate that by taking into account the Gouy phase of the mode $\Psi_{33}$ we need to obtain a multiple of six, that is, $\Delta\phi = 3\pi/6$. Thus $\psi_{(1,3)}$ acquires a global phase $\pi \pmod{2\pi} + 3\pi/6$ and $\psi_{(0,2,4)}$ a global phase $3\pi/6 \pmod{2\pi}$. Therefore, by introducing $\theta = -3\pi/6$, all the five modes are multiplexed forming a total optical field $\psi_0$.

Finally, it is convenient to indicate that LG modes of order $\mu = \nu$ are only obtained approximately, that is, the BP will also produce, by diffraction, other rotational symmetry modes ($\nu' = \mu'$). Let us suppose that residual modes $\hat{\Psi}_{00}$, $\hat{\Psi}_{11}$, $\hat{\Psi}_{22}$ and $\hat{\Psi}_{33}$ are generated simultaneously with $\Psi_{44}$. When $\Psi_{44}$ is multiplexed with $\Psi_{00}$, then $\hat{\Psi}_{00}$ and $\Psi_{00}$ exit the MZI by opposite ports, removing the crosstalk from the $\Psi_{44}$ input. Analogously when $\psi_{(0,4)}$ is multiplexed with $\Psi_{22}$, $\hat{\Psi}_{22}$ is not incorporated to $\psi_{(0,2,4)}$, and so on. In general, if a mode enters the MZI by a particular input and exits through a single port, then the same mode from any other input can not be output through the same port.

In short, the mentioned RPGSs only multiplex some of these LP modes, and simultaneously remove their crosstalk.

## 3. Refractive image inversion shifters

In the above section we have shown the limitations of the RGPSs when BPs are used and a $G(\pi)$ shifter is required. It is related to the generation of several HG modes by diffraction and the non-geometrical result $\Phi_{mn} = (m + n + 1)(\pi - \epsilon)$. This limitation can be avoided by using an exact image inverter, for example a RIIS. As we will show, the action of a RIIS is not only independent of the position of the BP (as in RGPS) but also of the half-width and curvature radius of the beam. This is a remarkable advantage for design and alignment. In addition, these shifters may produce diffracted modes closer to the modes of a FMF. Indeed, we have checked that an optical beam obtained by diffraction in a plate $BP_{11}$ (an Erfi-Gaussian mode) couples more than 80% of its power to the $LP_{11}$ mode of a step-index fiber. On the other hand, in a reflective inverter, the beam must be reflect an even number of times in an arm and an odd number in the other. Therefore, even assuming ideal metal reflections, there is a $\pi$ phase difference between both polarizations, which should be compensated with a birefringent phase plate to obtain a polarization-insensitive device. Furthermore, the path difference must be kept to zero, and not only due to coherence issues, as we will shown. This also complicates the path of the opposite arm [9]. Conversely, refractive inverters lack these added difficulties. Consequently, RIISs can become of a great interest and, therefore, very resorted, because there are many LP modes with $l \neq 0$ which can be multiplexed in this way.

### 3.1. Wave approach to exact image inversion

Here, instead of decompose the optical field as a combination of HG modes, we study directly the diffraction from the BP (object plane) by using the optical propagator, and next we compare the diffracted fields along both arms. So the complex amplitude distribution at a given plane (XY) can be expressed by

$$\Psi_e(\boldsymbol{\rho}) = \int\int K(\boldsymbol{\rho}, \boldsymbol{\rho}_0)\Psi_0(\boldsymbol{\rho}_0)d\boldsymbol{\rho}_0 \tag{17}$$

where $\Psi_0(\boldsymbol{\rho}_0)$ is the complex amplitude distribution at the object plane and the optical propagator $K(\boldsymbol{\rho}, \boldsymbol{\rho}_0)$ is given, except for non relevant complex constants, by Eq. (2). For the path 1 the ABDC matrix is now:

$$\begin{pmatrix} A_1 & B_1 \\ C_1 & D_1 \end{pmatrix} = \begin{pmatrix} 1 & d_e \\ 0 & 1 \end{pmatrix} \begin{pmatrix} \tilde{A}_1 & \tilde{B}_1 \\ \tilde{C}_1 & \tilde{D}_1 \end{pmatrix} \begin{pmatrix} 1 & d_0 \\ 0 & 1 \end{pmatrix}, \tag{18}$$

Optics EXPRESS

where $d_0$ is the distance from the BP to the first lens of the optical system and $d_e$ is the distance from the last lens to the plane XY. Let us consider that the optical system fulfills $A_1 = D_1 = -1$ and $B_1$ can be done as small as needed; then we can write Eq. (2) as follows

$$\lim_{\Delta\to 0} \frac{1}{\pi\Delta} \exp\left[-\frac{(x+x_0)^2 + (y+y_0)^2}{\Delta}\right] = \delta(x+x_0, y+y_0), \tag{19}$$

with $\Delta = -2B_1/ik_0$ and where we have used the definition of the Dirac delta function [19]. Now, from Eq. (17) we obtain $\Psi_e(x,y) = \Psi_0(-x,-y)$. Therefore, if $\Psi_0(x_0,y_0)$ is an odd function along $x$-direction and even along $y$-direction or vice versa we obtain the same amplitude distribution but the beam has acquired a relative phase $\pi$: $\Psi_e(x,y) = e^{i\pi}\Psi_0(x,y)$. Otherwise, if $\Psi_0(x_0,y_0)$ is an even function along $x$ and $y$-directions, then $\Psi_e(x,y) = \Psi_0(x,y)$, and so on. On the other hand, the condition $B_1 = 0$ provides the position of the image plane, that is, the plane where the optical propagator becomes a delta function. Now, as in the multiplexing with RGPSs, the maximum constructive interference at one of the outputs of the MZI is achieved by phase matching (except for a constant) of the amplitude distributions along both paths. This condition requires the matching of the BP image planes along both arms of the MZI. In particular, if the optical beam propagates freely in the arm 2, the optical system in the arm 1 must form a virtual image of BP on itself. Formally, the condition $d_e = -d_0 - d_1$ must be fulfilled, being $d_1$ the length of the optical system $\tilde{A}_1\tilde{B}_1\tilde{C}_1\tilde{D}_1$. When a selective action on each spatial direction is required, cylindrical systems should be used. In that case the optical propagator will only have an active direction, but similar results are obtained. For example, we need an image inversion in just one direction to multiplex the LG modes $\Psi_{01c} = \Upsilon_{10}$ and $\Psi_{01s} = \Upsilon_{01}$. Thus, if we use $x$-cylindrical lenses to implement a RIIS, the propagator becomes $\delta(x+x_0, y-y_0)$ and therefore the mode $\Psi_{01c}$ gains a phase $\pi$, but the mode $\Psi_{01s}$ does not, that is, at one of the outputs of the MZI we obtain the optical field $\Psi_{01c} + \Psi_{01s}$. The rotation of the cylindrical lenses to any angle is easier than mode rotation or rotation of the whole interferometer, which is an advantage with respect image inversion by mirrors. Alternatively, other refractive elements could be used, such as a Dove prism. However, in that case, the same problems of phase mismatch appear when a BP is used.

### 3.2. Designs of refractive image inverters

The image inverter is the central element of the MZI, therefore it is convenient to describe it in more detail. We present two implementations as in the RGPS case.

#### 3.2.1. RIIS with conventional lenses

In order to explain its operation let us begin by reconsidering the $G(\pi)$ shifter: two identical lenses $L_0$ and $L_2$ of focal length $f$, separated by a distance $d_1 = 2f$. In this case the matrix given by Eq. (18) is

$$\begin{pmatrix} A_1 & B_1 \\ C_1 & D_1 \end{pmatrix} = \begin{pmatrix} -1 & 2f - d_0 - d_e \\ 0 & -1 \end{pmatrix}. \tag{20}$$

There is a magnification $-1$ when $d_e = 2f - d_0$. Therefore, the distance between the object and the image plane is $4f$. That is, as seen from the BS2, the image of the plate is always inverted and seems closer than its direct image through the arm 2. Therefore, Fresnel diffraction undergone by the field in each arm of the MZI is quite different, which prevents a full destructive interference in one of the outputs for an arbitrary input field. We could enlarge the path 1 in an amount of $4f$ in order to adjust the diffraction, but this would worsen the coherence. The only way to compensate for this different diffractive effect in each arm is to use an optical system which produces an exact image inversion on the BP plane itself. One possible solution is to include a third lens $L_1$ of focal length $f_1$, located halfway between $L_0$ and $L_2$, as indicated in Fig. 3.

Optics EXPRESS

The optical matrix of this new inverter is also given by Eq. (20), except for the term $B_1$ which now is $2f - f^2/f_1 - d_0 - d_e$. The focal length $f_1$ is a new freedom degree that allow us to simultaneously meet $B_1 = 0$ and $d_e = -d_0 - 2f$, by selecting $f_1 = f/4$. In short, according to Eqs. (2) and (19), the optical system produces an image inversion located virtually on the BP regardless its position and the curvature or width of the beam. This makes easier the mounting of the inverter system. Alternatively, and for sake of completeness, Fig. 3 shows a ray tracing of the image inverter with three lenses. The object focal point $F_0$ and the image focal points $F_1'$ and $F_2'$ are indicated for facilitating the ray tracing. Finally, we will denote this RIIS as $I_\pi$. The cylindrical RIIS will be denoted as $I_{\pi\eta}$, with $\eta = x, y$.

#### 3.2.2. RIIS with graded-index lenses

In this case we will use two optical systems, one in each arm of the MZI. Let us consider a 1/2-pitch graded-index lens in the path 1 of the MZI, that is, $g_{o1}l = \pi$ and a 1-pitch graded-index lens of the same length $l$ in the path 2 of the MZI, that is, $g_{o2}l = 2\pi$. By taking into account the matrix of a graded-index lens, presented in section 2, the optical propagators are given by

$$K^{(1)}(\boldsymbol{\rho}, \boldsymbol{\rho}_0) = \frac{ik_0}{2\pi d} \exp\left[\frac{-ik_0}{2d}(\boldsymbol{\rho} + \boldsymbol{\rho}_0)^2\right] \tag{21}$$

$$K^{(2)}(\boldsymbol{\rho}, \boldsymbol{\rho}_0) = \frac{ik_0}{2\pi d} \exp\left[\frac{-ik_0}{2d}(\boldsymbol{\rho} - \boldsymbol{\rho}_0)^2\right] \tag{22}$$

with $d = d_0 + d_e$, being $d_0$ and $d_e$ refereed to the faces of the lenses. If $d_e = -d_0$ then the optical propagators become $\delta(x + x_0)\delta(y + y_0)$ and $-\delta(x - x_0)\delta(y - y_0)$. Thus, virtual images are obtained at the same distance from BS2 and the diffraction is the same in both arms of the MZI. In addition, the first graded-index lens introduces a phase $\pi$, which is needed to multiplex modes with opposite parity.

### 3.3. Multiplexing of LG modes with $\nu > \mu$

Finally, we present an example of multiplexing of LG modes with $l \neq 0$, in particular, we will multiplex $\Psi_{10s}$, $\Psi_{10c}$, $\Psi_{20s}$, $\Psi_{20c}$ and the optical field $\psi_0$ formed by the five modes $\Psi_{mm}$ ($m = 0, 1, 2, 3, 4$), multiplexed by RGPSs in the above section. We start by multiplexing the optical field $\psi_0$ and the mode $\Psi_{20c}$ to obtain $\psi_{(0,20c)} = \psi_0 + \Psi_{20c}$. For that, we need a $G_{x'}(\pi/2)$

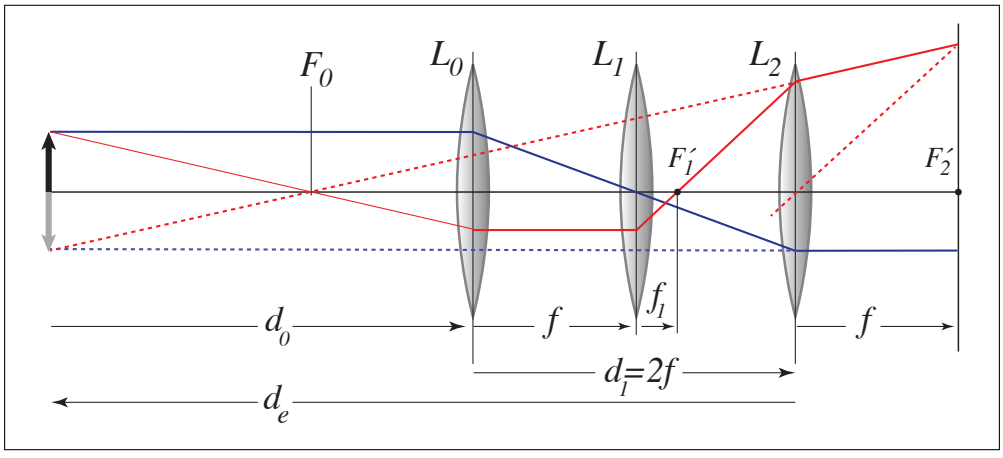


Fig. 3. Sketch of the refractive image inverter and ray-tracing.

Optics EXPRESS

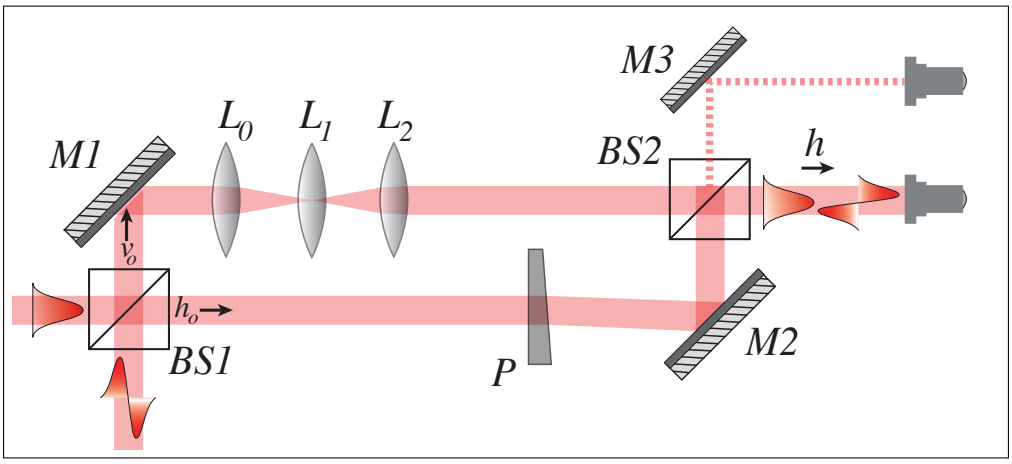


Fig. 4. Sketch of the MZI with refractive inverter $L_0L_1L_2$.

shifter, being $x'y'$ a rotated reference system with $x' = (x + y)/\sqrt{2}$ and $y' = (-x + y)/\sqrt{2}$. As $\psi_{(0,20c)}$ is even, it can be multiplexed with the odd mode $\Psi_{10c}$ by using a $I_\pi$ shifter; that is, we obtain $\psi_{(0,20c,10c)} = \psi_{(0,20c)} + \Psi_{10c}$. On the other hand, the odd mode $\Psi_{10s}$ and the even mode $\Psi_{20s}$ are multiplexed with other $I_\pi$ shifter, which results in an odd function along $y$ direction: $\psi_{(10s,20s)} = \Psi_{10s} + \Psi_{20s}$. Finally, $\psi_{(10s,20s)}$ can be combined with the even function on $y$ ($\psi_{(0,20c,10c)}$) by using a $I_{\pi y}$ shifter. Thus, we obtain the total field $\psi_T = \psi_{(10s,20s)} + \psi_{(0,20c,10c)}$ which comprises 9 modes. These multiplexing optical systems remove the crosstalk that the BPs can generate in the LG modes, in the same way that MZIs with RGPSs do.

## 4. Experimental results and analysis

We show in Fig. 4 a sketch of a MZI used in an experiment of bimodal multiplexing. A picture of the corresponding setup is shown in Fig. 5. Each input port of the MZI is illuminated with a He-Ne laser beam ($\lambda = 633$ nm). An arm of the MZI includes a RIIS consisting of three lenses $L_0$, $L_1$ (field lens) and $L_2$. In particular, two achromatic doublets of focal lengths $f_0 = f_2 = f = 4$ cm, and a Plössl eyepiece (two achromatic doublets) of focal length $f_1 = 1$ cm. The other arm has a thin prism P to adjust the phase $\theta$ to an integer value of $\pi$, by moving it perpendicular to the optical axis. We achieve a finer optical path compensation in this way that, for example, by translating a mirror. The MZI is placed on an optical table with pneumatic vibration isolators in order for it to be stable. Other factors such as drafts or temperature changes can affect the performance of the system but they are easily controllable. Next, we present experimental results on multiplexing of $\Psi_{00}$ and $\Psi_{10c}$ modes, hereafter denoted by the standard notation of LP modes, $LP_{01}$ and $LP_{11}$. The first mode is obtained from the laser beam that enters trough the $h_0$ input of the MZI. The mode $LP_{11}$ is generated by using an slightly expanded laser beam incident on a phase plate $BP_{11}$ placed at the input $v_0$ of the MZI (not shown in Figs. 4 and 5). The beam expansion is not essential, but by one hand it facilitates the determination of conjugated planes in order to fit the optical elements, and on the other hand, it ensures, in relative terms, that the transition region of the phase plate acts as an quasi-abrupt border since it is not strictly so (about 10 $\mu$m width). We must note that this mode is actually an Erfi-Gaussian mode and that the BP used have been fabricated by ion-exchange technology in glass [5]. As commented, this technology stands out because of its high versatility and precision, enabling the production of monolithic, uniform and robust phase plates. Finally, the optical modes at the output of the MZI are collected on two photodetectors or a screen to be photographed. We analyze the outputs

Optics EXPRESS

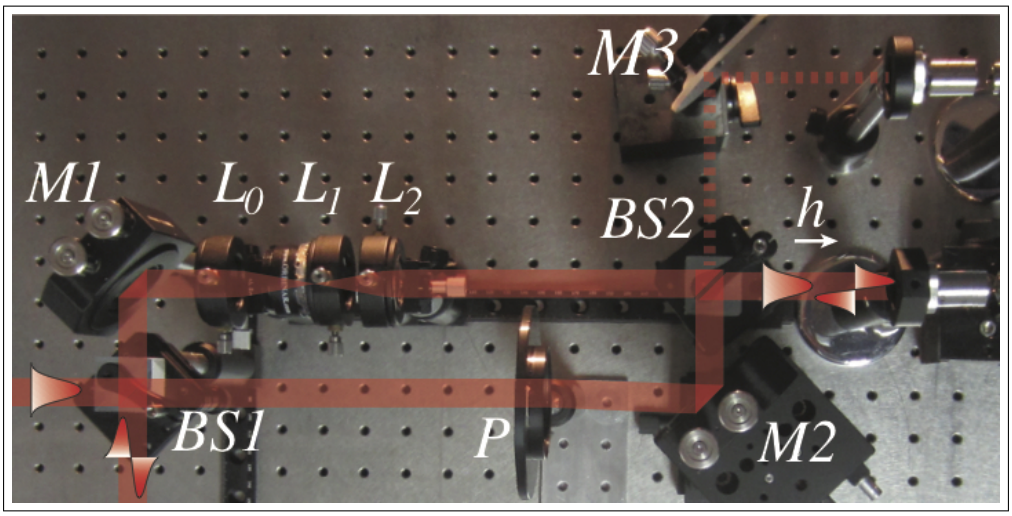


Fig. 5. Photography of the MZI used in the experiment.

Table 1. Optical power values at $h$ and $v$ outputs of the MZI.

| | | RIIS | | RGPS $G(\sim \pi)$ | |
|---|---|---|---|---|---|
| Mode | $\theta$ | $P_h$ ($\mu$W) | $P_v$ ($\mu$W) | $P_h$ ($\mu$W) | $P_v$ ($\mu$W) |
| $LP_{01}$ | $2m\pi$ | 7140 ± 50 | 220 ± 20 | 7990 ± 50 | 150 ± 20 |
| $LP_{11}$ | $2m\pi$ | 6550±50 | 200 ± 20 | 7415 ± 50 | 440 ± 20 |
| $LP_{01}$ | $(2m+1)\pi$ | 230 ± 20 | 6420 ± 50 | 200 ± 20 | 6900 ± 50 |
| $LP_{11}$ | $(2m+1)\pi$ | 230 ± 20 | 5600 ± 50 | 525 ± 20 | 6325 ± 50 |

of the MZI by blocking the $h_0$ or $v_0$ input. After the adjustment of the phase $\theta$, the power measurements $P_h$ and $P_v$ corresponding to the $h$ and $v$ outputs, respectively, were carried out in order to evaluate the efficiency of derivation of the interferometer. By blocking the $v_0$ input a Gaussian mode is obtained at the output $h$, although a small amount of light is measured at the $v$ output. Next, by blocking the $h_0$ input an Erfi-Gaussian mode is also obtained at the output $h$, and again a small amount of light is measured at the $v$ output.

The results of these power measurements are collected in the central columns of Table 1 for the two modes separately and under phase shifts $\theta$ with even and odd values of $\pi$. In all cases, an average demultiplexing efficiency of about 96.5% is reached. The 3.5% average of inefficiency must be attributed primarily to non-paraxial effects of the elements, different reflective losses in each arm, and finally, spatial modal noise of the input beams, since they were not spatially filtered, leading to deviations of the modal amplitude from a totally even or odd function. Obviously, the first way to reduce such losses is the use of refractive elements (prism, lenses and objectives) having good anti-reflective coatings, and the use of dielectric mirrors and beam-splitters instead of metallic ones. Moreover, the use of a mode from an optical fiber as a light source will improve the spatial beam quality (more symmetrical) respect the non-spatially filtered laser beams. Likewise, the lenses introduce a small amount of aberrations that prevents a simultaneous destructive interference across the whole wavefront. Better corrected lenses will improve that, mainly if expanded beams are used.

In the columns 5 and 6 of Table 1 we also show the results obtained without lens $L_1$, that

Optics EXPRESS

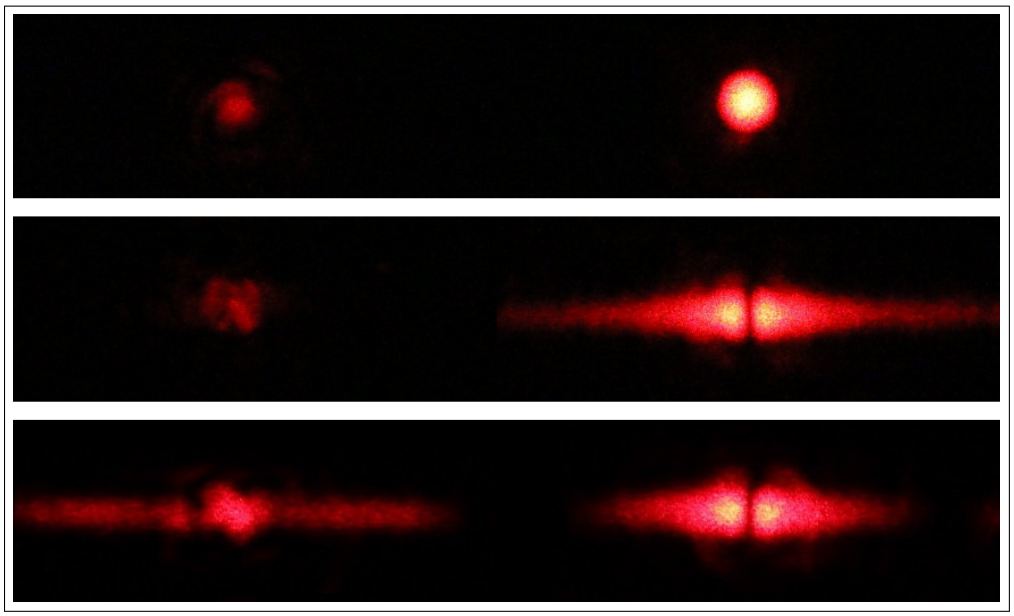

Fig. 6. Images of the modes at outputs $v$ (left) and $h$ (right) for a RIIS (top and middle) and a RGPS $G(\sim \pi)$ (bottom).

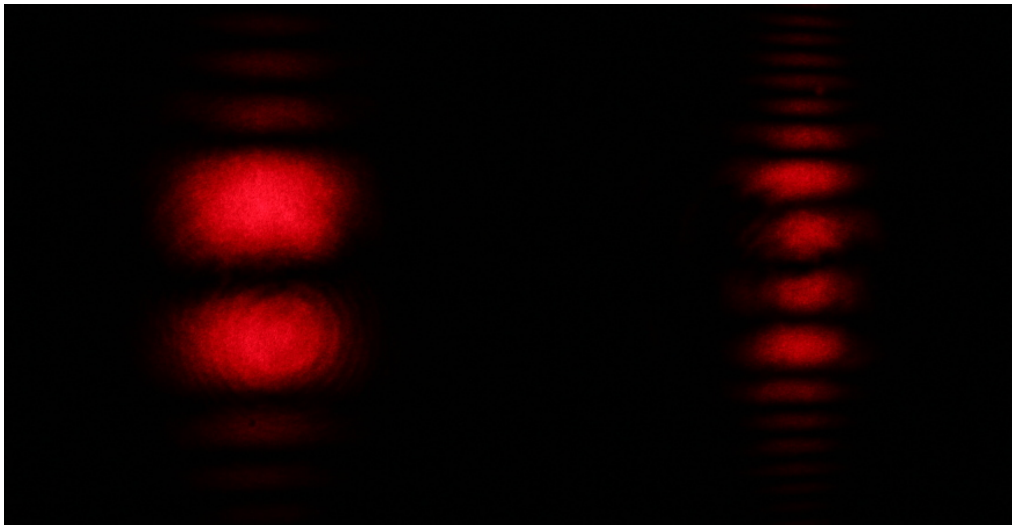

Fig. 7. Images of the outputs $v$ (left) and $h$ (right) for a $G(\pi/2)$ RGPS.

is, with a RGPS G($\sim \pi$). Note that the power values for destructive interference of mode $LP_{11}$ (row 2, column 6 and row 4, column 5) have increased respect to the corresponding values for a RIIS (same rows, columns 4 and 3 respectively), which justifies the advantage of using a RIIS. We must stress again that the lens $L_1$ has a poor transmittance for 633 nm which reduces the visibility of the interference (compare destructive interferences of the mode $LP_{01}$ in both systems). Therefore, even better values of RIIS would be easily obtained by using a $L_1$ lens with a proper anti-reflective coating.

A picture of the intensities of the $LP_{01}$ and $LP_{11}$ modes at the outputs of the MZI is presented

Optics EXPRESS

in Fig. 6. The images are slightly saturated on their right side so that the other output (left) can be observed. At the top of the picture only the even mode was registered by blocking the $v_0$ input; at the middle the mode $LP_{11}$ (generated by $BP_{11}$) was recorded by blocking the input $h_0$. In both cases, some energy is observed at the other output (left), which corresponds to the losses of 3.5% measured. To take the photograph below, the input $h_0$ remained blocked, and the lens $L_1$ was removed so that $L_0$ and $L_2$ lenses worked as a RGPS $G(\sim \pi)$. The increase in losses at the output $v$ (left) is clear. This is due to coupling to high order HG modes as discussed above.

Finally, a $G(\pi/2)$ RGPS was implemented by several changes in the system. The distance between $L_0$ and $L_2$ was set at 57 mm according to Eq. (8) with $\Delta\phi = \pi/2$. The illumination beam (from the $v_0$ input port) was adjusted to be convergent with Rayleigh distance equal to $z_{R2} = d/\kappa = 68.3$ mm (full angle beam convergence 3.5 mrad). Moreover, the beam waist was placed midway between $L_0$ and $L_2$. The $BP_{11}$ plate was used to generate the $\Upsilon_{01}$ mode as well as the unwanted odd modes $\Upsilon_{03}$, $\Upsilon_{05}$... The phase compensator $\theta$ was adjusted to minimize the right output power ($h$ port) of Fig. 7. On the left side we can see two lobes corresponding to the $\Upsilon_{01}$ mode while the four central lobes of the right side are due to the $\Upsilon_{03}$ mode, as expected from Eq. (8) since $\Phi_{03} - \Phi_{01} = \pi$. Similarly, $\Upsilon_{05}$, $\Upsilon_{09}$... exit through the $v$ port together $\Upsilon_{01}$ and $\Upsilon_{07}$, $\Upsilon_{0,11}$... do through the $h$ one, giving residual interferences in the tails of both outputs. This result proves experimentally the interferometric demultiplexing of $\Upsilon_{01}$ and $\Upsilon_{03}$ modes, being both of them odd along $y$ direction and even along $x$ direction. This operation is impossible with image inverters. On the other hand, this system can become a multiplexer if a $\Upsilon_{03}$ mode is introduced by the $h_0$ input port. This new mode will also exit through $v$ port together the $\Upsilon_{01}$ mode. In addition, as the former $\Upsilon_{03}$ mode from $h_0$ input port was sent by the interferometer to $h$ output, crosstalk between both $\Upsilon_{03}$ modes is avoided.

## 5. Conclusions

We have presented two kinds of phase shifters for space mode multiplexing with modes generated by binary phase plates. We have shown both theoretically and experimentally that modes with same parity can be multiplexed by using Gouy phase shifters (RGPS). They have been used to multiplex the first five radial Laguerre-Gaussian modes, that is, with $\nu = \mu$. Next, we have presented refractive exact image inverters (RIIS), that is, optical systems producing virtual image inversion at the plane of the binary phase plate generating the optical mode. This assures an efficient interferometric multiplexing. RIIS can be used to multiplex four additional non-radial modes ($\nu \neq \mu$), giving a total of nine modes. Likewise, we have proven experimentally that a RGPS that shifts selectively $\pi/2$, that is, a $G(\pi/2)$ demultiplexes two odd modes, which can not be achieved by any image inverter. We have predicted theoretically that both kinds of interferometers remove the crosstalk generated by the binary plates in the LG modes, simultaneously to the multiplexing function. We must stress that the experimental results corresponding to the RGPS $G(\pi/2)$ have confirmed such a prediction. We have shown that all above phase shifters are polarization-insensitive, have a small footprint and can easily act in any direction using cylindrical lenses or both using spherical lenses. Moreover, they can be implemented by using both conventional and graded-index lenses. The latter being highly compatible with optical fibers. Finally, we have checked in an experimental way the interferometric multiplexing of the modes $LP_{01}$ and $LP_{11}$, in such a way that about 96.5% of the output power is in the desired port. Moreover, we have proven experimentally that a simple RGPS $G(\sim \pi)$ provides worse results by removing the central lens of a RIIS.

## Funding

Ministerio de Economía y Competitividad, Central Government of Spain, Contract number FIS2013-46584-C2-1-R; Fondo Europeo de Desenvolvemento Rexional 2007-2013 (FEDER).